536.423.1::532.542

Paper No. 191-10

Prediction Method of Flow Patterns in Subcooled and Low Quality Boiling Regions*

By Kotohiko SEKOGUCHI**, Osamu TANAKA***, Shuji ESAKI†, Noriaki KATSUKI††, Masao NAKASATOMI†††

A new parameter is proposed for prediction of the transition between flow patterns such as bubble, froth and annular flow, in both the subcooled and low quality regions of boiling flow. This parameter is derived from the theoretical calculation method of void fraction, which has been reported, on the assumption that the flow pattern transition occurs at a value of average void fraction over the cross section of the flow. A flow map is also presented which reasonably correlates the experimental results covering the following conditions ; pressure : 1∿98 ata, heat flux : $2\times10^4\sim5\times10^6$kcal/m^{2}h, and mass velocity : 40∿5400kg/m^{2}s.

1. Introduction

A knowledge of flow patterns such as bubble, slug, froth and annular flow is of vital importance in understanding the phenomena associated with boiling two-phase flow. The need for predicting flow patterns in subcooled and saturated boiling regions has led to numerous experimental investigations. Flow patterns in two-phase flow were first classified by visual observation of the flow, in which still and/or cine photography were used. Visual techniques are inevitably not only subjective, but unavailable to the central subchannel flow in tube bundle; thus, some instrument techniques have been proposed for quantitative determination of flow regimes or flow type boundaries. In case of boiling flow, usual flow systems are operated at elevated pressures and a special pressure window is necessary for observation. However, using the electrical void probe method[3]~[6], the flow patterns even inside a heated tube made of metal can be identified by the characteristics in phase distributions.

It is specially noticed in boiling flow with subcooling that there appears not only bubble flow but froth flow in the subcooled boiling region depending upon the thermal-hydrodynamic condition. As would be expected, the prediction of such a variety of flow patterns in the subcooled region is closely related to the evaluation of true steam quality or void fraction.

A large number of studies have been carried out for the evaluation of true quality or void fraction[1],[2],[16]~[28]. As a result of these studies, the governing parameters are supposed to be pressure, heat flux, mass velocity, channel size and thermal equiliblium quality. In contrast to this, the existing flow map usually used for boiling flow correlates only two parameters, i.e., mass velocity and thermal equilibrium quality[3]~[8]. A more comprehensive flow map, therefore, should be developed to evaluate every parameter.

Experiments of adiabatic air-water two-phase flow reveal that the transition between bubble and froth flow usually occurs at a cross-sectional average void fraction of 20% to 30%[10], but under a certain condition a bubble flow can be observed at an average void fraction of 45%, and at a local void fraction of 58%[9]. However, experimental results of boiling flow[11] indicate a possibility of uniquely predicting the transitions between bubble, froth, and annular flow by the average void fraction.

Based on the latter experiments, the average void fraction is employed here as an index of the transition of flow patterns, and a parameter correlating the true quality is introduced to produce a more general flow map. The experimeatal data used for the map are as follows; pressure: 1∿98 ata, heat flux: $2\times10^4\sim5\times10^6$ kcal/m^{2}h, and mass velocity; 40∿5400kg/m^{2}s.

2. Notations

- Bo : boiling number (=q/G h_{fg})
- Bo*, Bo$^+$: modified boiling numbers defined by Eqs.(12) and (13), respectively
- c_p : specific heat of liquid at constant pressure, kcal/kg°C
- D : pipe diameter, m or mm
- D_e : equivalent diameter, m or mm
- G : mass velocity, kg/m^{2}s
- h : specific enthalpy, kcal/kg

* Received 17th August, 1979.

** Professor, Faculty of Engineering, Kyushu University, Fukuoka, Japan.
*** Research Assistant, Faculty of Engineering, Kyushu University, Fukuoka, Japan.
† Post Graduate Student, Faculty of Engineering, Kyushu University, Fukuoka, Japan.
†† Engineer, Ryonetsu Company, Fukuoka, Japan.
††† Professor, Ube Technical College, Ube, Japan.

h_f : specific enthalpy of liquid at saturation temperature, kcal/kg
h_{fg} : latent heat of vaporization, kcal/kg
$\tilde{h}_{sp}$: heat transfer coefficient difined by Eq.(5), kcal/m^{2}h°C
k : thermal conductivity of liquid, kcal/mh°C
Km, Kn : constants difined by Eqs. (4) and (3) respectively
m,n : exponents in Eqs.(2) and (1) respectively
p : pressure, ata
p_c : critical pressure, ata
Pr : Prandtl number
q : heat flux, kcal/m^{2}h
R : pipe radius, m or mm
Re : Reynolds number (=Du/ν)
T : temperature, °C
T_b : bulk temperature, °C
T_c : temperature at center line, °C
T_s : saturation temperature, °C
T_w : temperature of heated wall, °C
T_{wexp} : experimental temperature of heated wall, °C
u : liquid velocity, m/s
u_c : liquid velocity at center line, m/s
u_{in} : inlet liquid velocity, m/s
x : thermal equilibrium quality
x_a : true vapor quality
y : distance from wall, m or mm
y* : dimensionless distance from wall (=y/R)
α : local void fraction
$\hat{\alpha}$: average void fraction over cross section of flow channel
μ : viscocity, kgs/m^2
ν : kinematic viscosity, m^2/s
ρ_g : mass density of vapor, kgs^2/m^4
ρ_ℓ : mass density of liquid, kgs^2/m^4
ψ : ratio of the mass of liqud flowing in homogeneous mixture to total mass of liquid flowing (defined by Eq.(14))

3. Determination method of flow patterns based on the characteristics of phase distribution

Void fraction distributions in both radial and axial directions were obtained at elevated pressures using the electric resistivity probe technique. The determination method of flow patterns estimated from the characteristics of the phase distribution is described below.

Typical examples of radial void fraction distributions are shown in Figs.1 (a), (b) and (c) for three pressures respectively[12],[13]. The test section used in Fig. 1 (a) is a cupronickel pipe of 15.78 mm i.d., 19.08 mm o.d. and 4.5 m long. Electrical probes are attached to four axial locations (i.e., 0.65 m, 1.85 m, 3.05 m and 4.25 m from the starting section of heating). Every probe can be traversed in radial direction. Local void fractions shown in Fig.1 (a) were measured for pressure P: 1.96 ata, heat flux q: 16.3×10^4 kcal/m^{2}h and mass velocity G: 695 kg/m^{2}s. Then the desired value of thermal equilibrium quality x was attained by varying the

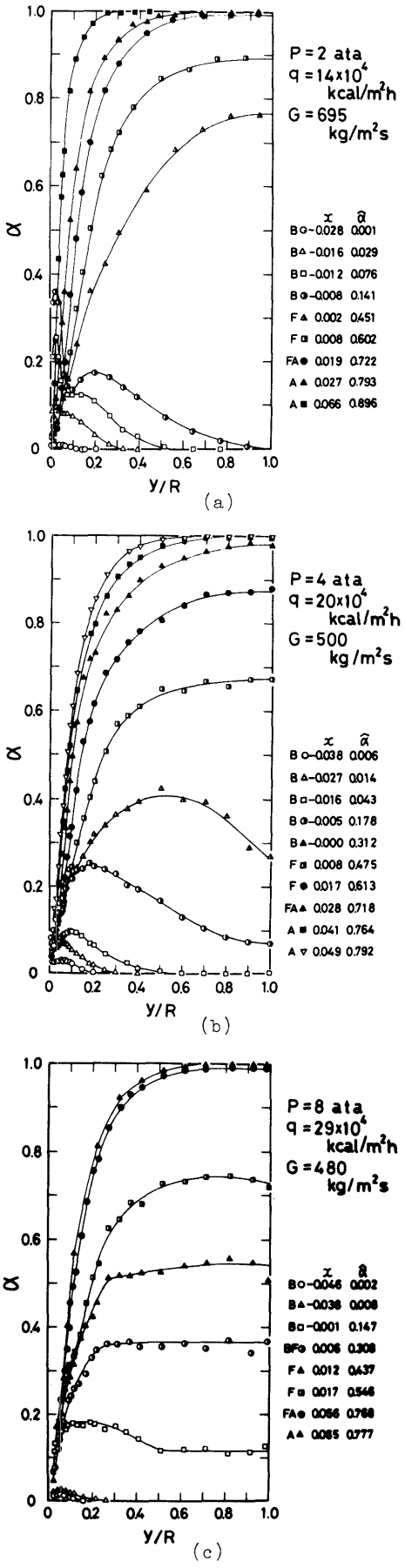

Fig.1 Void fraction distribution in boiling flow

inlet subcooling. The test section used in Figs. 1 (b) and (c) was also made of cupronickel and with dimensions: 13.55 mm i.d., 15.90 mm o.d. and 2.09 m long. The experimental conditions were pressure: 4 and 8 ata, heat flux: 20×10^4 and 29×10^4 kcal/m^{2}h, mass velocity: 500 and 480 kg/m^{2}s. Average void fraction $\hat{\alpha}$ obtained by integrating the local void fraction over the cross-sectional area and flow patterns (B: bubble flow, BF: transition from bubble to froth flow, F: froth flow, FA: transition from froth to annular flow, A: annular flow) are shown in Figs. 1 (a) through (c). The void fraction except for a specific zone close to the heated surface increases as thermal equilibrium quality increases in the flow direction. The existence of a maximum void fraction near the heated surface characterizes the two-phase flow in both the surface boiling region and the beginning region of the pseudo-saturated boiling, for example, symbols "○", "△" and "□" in Fig. 1 (b). In the surface boiling region, vapor bubbles repeatedly grow and vanish on the heated surface, and sometimes leave the boiling sites and slide on the wall ; while in the pseudo-saturated boiling region, bubbles can grow up to vapor slug and depart from the heated surface. Further, when thermal equilibrium quality is increased, the existence of bubbles can be recognized at the center of the tube and the maximum void fraction point moves toward the center (symbols "◑" and "▲" in Fig. 1 (b)). Data of the simbol "▲" in Fig. 1 (b) indicate that the local void fraction at the center is 27% and a void fraction peak is not yet recognized at the center of the tube. The void fraction for the symbol "◑" in Fig. 1 (c) takes a maximum (36%) at the center of the tube. This is probably caused by a frequent appearance of vapor slug. From a point of view described above, examining our 22 experimental data, it is found that the void fractions falling between about 30% and 50% at the center could be expected to correspond to the transition from bubble to slug or froth flow. In general, if the void fraction at the center line exceeds about 50%, the maximum of void fraction always occurs at the center of the tube. At higher thermal equilibrium qualities, vapor slugs rapidly grow up and coalesce into a vapor column. The flow pattern transition from froth to annular flow starts at the void fraction of about 95% at the center and finishes at about 100%.

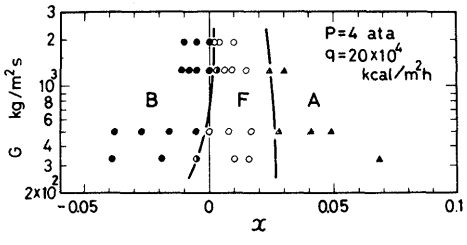

Fig.2 An example of typical flow pattern map for boiling flow

On the basis of the measured radial void profiles, the flow patterns in boiling flow are classified as follows;
(1) Bubble flow : Maximum void fraction occurs near the heated wall, and the void fraction at the center line of the pipe, α_c, is lower than 30%.
(2) Transition from bubble to froth flow : Maximum void fraction point moves toward the center line, and α_c is higher than 30% and lower than 50%.
(3) Froth flow : Maximum void fraction appears at the center line, and α_c is higher than 50% and lower than 95%.
(4) Transition from froth to annular flow : α_c is higher than 95%.
(5) Annular flow : α_c is 100%.

4. Existing prediction method of flow patterns in subcooled region of boiling flow

In order to compare the transition boundaries from one particular regime to another in a subcooled boiling flow with those in an adiabatic gas-liquid two-phase flow, it is necessary to evaluate the effect of subcooling upon the vapor flow rate, because most flow maps for adiabatic systems are drawn with the parameters including the gas-phase flow rate. However, flow patterns of a boiling flow have been mapped on a diagram of mass velocity, G, against thermal equilibrium quality, x, for the pressure of the flow system.[3)-7),7),8)]

Such an example of the G vs. x-map is shown in Fig.2, where flow regimes are specified from the experimental results of the radial distribution of void fractions based on the classification mentioned above. The transition boundary from bubble to froth flow gradually shifts toward the smaller thermal equilibrium quality with decreasing mass velocity.

Next, the effect of the heat flux on the transition boundaries is shown in Fig.3. From this figure, it is found that the transition between froth and annular

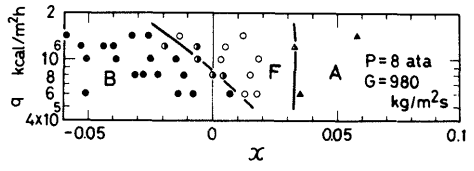

Fig.3 Flow pattern map q vs. x

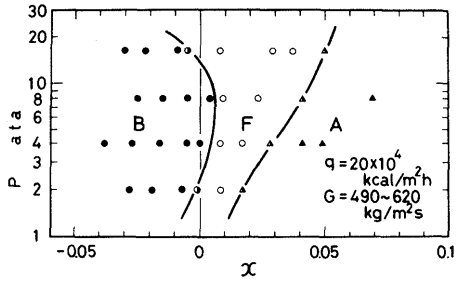

Fig.4 Flow pattern map on P vs. x

flow is hardly affect by the heat flux but the transition boundary from bubble to froth flow greatly changes from the saturation to the subcooling zone with an increasing heat flux. The system pressure is selected as another parameter considered to affect the transition, and an example of the map is given in Fig.4.

Since the transition boundaries are definitely linked with heat flux and system pressure as seen in Figs.3 and 4, the usual flow map on G vs. x made at a test condition of heat flux and pressure is not always effective under other conditions. Thus, a more general flow map is needed including various important parameters.

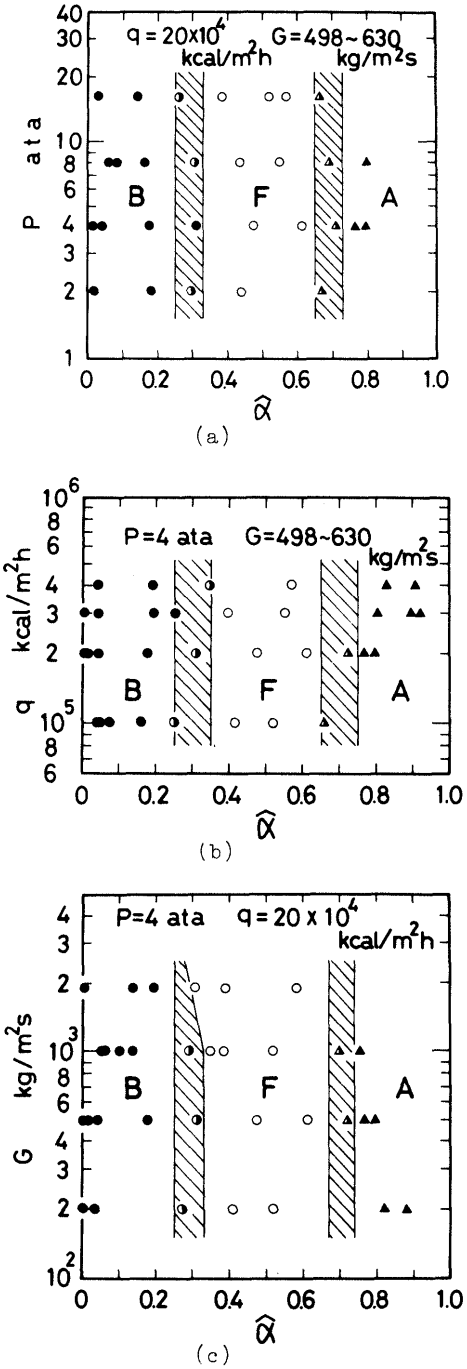

Fig.5 Flow pattern map on P vs. $\hat{\alpha}$

5. New parameter for correlating transition boundaries of flow patterns

Jones and Zuber[14] proposed a method for prediction of flow patterns in an air-water two-phase flow ; i.e., using the average void fraction $\hat{\alpha}$, flow patterns were divided into three categories such as bubble flow ($\hat{\alpha}<0.2$), slug flow ($0.2<\hat{\alpha}<0.8$)and annular flow ($\hat{\alpha}<0.8$). On the other hand, authors obtained the average void fractions in a steam-water boiling flow at elevated pressures. Using our data on the average void fractions of a boiling flow at elevated pressures, flow patterns are mapped as in Figs.5(a) through(c), where the average void fraction is on the abscissa, and pressure, mass velocity, and heat flux are on the ordinate, respectively. These results reveal that flow patterns are roughly governed only by the average void fraction ; i.e., bubble flow ($\hat{\alpha}<0.3$), froth flow, corresponding to slug flow defined by Jones and Zuber, ($0.3<\hat{\alpha}<0.7$), and annular flow ($\hat{\alpha}<0.7$).

Thus, the average void fraction is used for prediction of flow patterns. The average void fraction in boiling flow under both subcooled and saturated conditions depends on pressure, heat flux, mass velocity, channel dimension, and physical properties of fluids. A new parameter correlating these variables with the average void fraction is proposed on the basis of an analytical model presented in previous report[2] for determining the void fraction.

The analytical model was set up from the experimental fact that the measured radial temperature profile in the flow core region is consistent with that of the single-phase flow and the superheated layer on the wall is extremely thinner than that for a single-phase flow, which is shown by way of explanation in Fig.6. The amount of

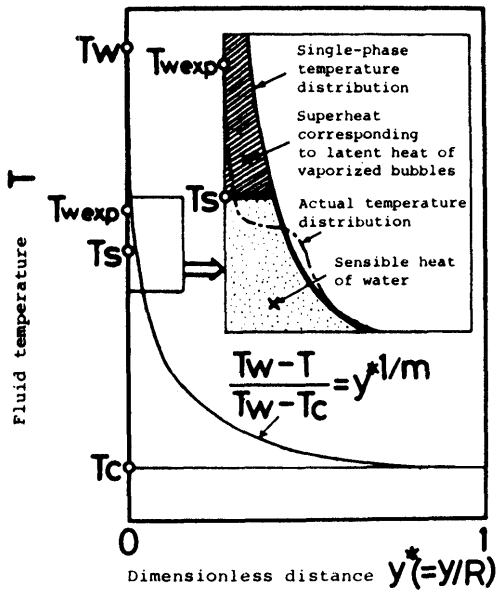

Fig.6 Physical model for temperature distribution in subcooled boiling flow

vapor flowing through a cross section of the tube is assumed to correspond to the heat quantity for superheat which is determined by extending the temperature curve for an imaginary single-phase flow.

The distributions of velocities and temperatures are expressed according to the power law as

$$\frac{u}{u_c}=\left(\frac{y}{R}\right)^{1/n}=y^{*1/n} \quad \cdots\cdots(1)$$

$$\frac{T_W-T}{T_W-T_c}=\left(\frac{y}{R}\right)^{1/m}=y^{*1/m} \quad \cdots\cdots(2)$$

where u and T are the local liquid velocity and temperature, u_c and T_c are the values at the center line, T_W is the wall temperature, and $y^*(=y/R)$ is a dimensionless distance from the wall.

Integrating Eqs.(1) and (2), the liquid mean velocity at the inlet u_{in} and the bulk temperature T_b can be expressed by

$$\frac{u_{in}}{u_c}=\frac{2n^2}{(n+1)(2n+1)}=K_n \quad \cdots\cdots(3)$$

$$\frac{T_W-T_b}{T_W-T_c}=\frac{m^2(n+1)(2n+1)}{(mn+m+n)(2mn+m+n)}=K_m \quad \cdots\cdots(4)$$

The wall temperature for single-phase T_W is obtained by means of the following heat transfer coefficient $\tilde{h}_{sp}$ which is evaluated by taking into account the increase of liquid velocity with an increased void fraction.

$$\tilde{h}_{sp}=\frac{q}{T_W-T_b}=0.023\frac{k}{D_e}\left(R_e\frac{1-x_a}{1-\hat{\alpha}}\right)^{0.8}P_r^{1/3} \quad \cdots\cdots(5)$$

where q is the heat flux, k is the thermal conductivity of liquid, D_e is the equivalent diameter, R_e and Pr are the Reynolds and Prandtl number, $\hat{\alpha}$ is the average void fraction, and x_a is the true vapor quality in subcooled flow boiling. Thermal equilibrium quality is described as

$$x=\frac{h-h_f}{h_{fg}}=\frac{c_p(T_b-T_s)}{h_{fg}} \quad \cdots\cdots(6)$$

where h and h_f are the enthalpies of a two-phase mixture and of a liquid at saturation temperature, h_{fg} is the latent heat of vaporization, c_p is the specific heat of liquid at constant pressure, and T_s is the saturation temperature. From Eqs.(2), (4),(5) and (6) the single-phase temperature distribution at a thermal equilibrium quality x is given by

$$T=\left(1-\frac{1}{K_m}y^{*1/m}\right)\frac{q}{\tilde{h}_{sp}}+\frac{h_{fg}}{c_p}x+T_s \quad \cdots\cdots(7)$$

Under the assumption that the true vapor quality x_a can be expressed as the ratio of the vapor mass flow rate generated by dissipation of the superheat of liquid to the total mass flow rate.

$$x_a=\frac{c_p\int_0^{y_s^*}(T-T_s)u(1-y^*)dy^*}{h_{fg}\int_0^1 u(1-y^*)dy^*} \quad \cdots\cdots(8)$$

where y_s^* is a dimensionless distance from the wall to the position with saturation temperature of the single-phase temperature profile. If the exponents m and n in Eqs. (1) and (2) are taken as 7.0, from Eqs.(1), (3) and (7), Eq.(8) becomes

$$x_a=B_0^*\left\{\frac{2}{7}y_s^{*(9/7)}-\frac{3}{35}y_s^{*(16/7)}\right\} \quad \cdots\cdots(9)$$

From Eq.(7)

$$y_s^*=\left\{\frac{5}{6}\left(1+\frac{x}{B_0^*}\right)\right\}^7 \quad \cdots\cdots(10)$$

Therefore, Eq.(9) can be rearranged as

$$x_a=B_0^*\left[\frac{2}{7}\left\{\frac{5}{6}\left(1+\frac{x}{B_0^*}\right)\right\}^9-\frac{3}{35}\left\{\frac{5}{6}\left(1+\frac{x}{B_0^*}\right)\right\}^{16}\right] \quad \cdots\cdots(11)$$

where

$$B_0^*=\frac{qc_p}{h_{fg}\tilde{h}_{sp}}=B_0^+\left(\frac{1-\hat{\alpha}}{1-x_a}\right)^{0.8} \quad \cdots\cdots(12)$$

$$B_0^+=B_0\left(\frac{c_p\mu^{0.8}g^{0.8}}{0.023kP_r^{1/3}}\right)(GD_e)^{0.2} \quad \cdots\cdots(13)$$

There are a number of correlations of void fraction available in the literature. As a result of comparison between our data and those calculated by the correlations, Smith's correlation[15] is employed, which is given by

$$\hat{\alpha}=\left[1+\frac{\rho_g}{\rho_l}\psi\left(\frac{1}{x_a}-1\right)+\frac{\rho_g}{\rho_l}(1-\psi)\left(\frac{1}{x_a}-1\right)\times\left\{\frac{\rho_l/\rho_g+\psi(1/x_a-1)}{1+\psi(1/x_a-1)}\right\}^{1/2}\right]^{-1} \quad \cdots\cdots(14)$$

where ψ is the ratio of the liquid flow rate as a homogeneous mixture to the total liquid flow rate, and Smith recommended 0.4 as the value of ψ.

From Eq.(14) the average void fraction $\hat{\alpha}$ is related to the true vapor quality x_a at a given pressure. Equation (11) gives x_a as a function of Bo* and x. From Eq.(12) Bo* is evaluated by Bo^+, $\hat{\alpha}$ and x_a. Finally $\hat{\alpha}$ can be obtained from Bo^+, x, and pressure. Consequently a family of constant average void fraction curves for a given pressure can be expressed on the diagram of Bo^+ against x. In the following section, the flow map for both the subcooled and saturated boiling regions will be obtained using the new parameter Bo^+ defined by Eq.(13), including the heat flux, mass velocity and equivalent diameter.

6. Results and discussion

Experimental results available in the literature and our data are plotted on the diagram of Bo^+ against x in Fig.7(a)~(g). The constant average void fractions are also expressed by dotted lines. The ranges of the experimental conditions are listed in Table 1 together with the channel geometry and the determination technique of the flow pattern. The experimental conditions covered by the present study are pressure: 1~98 ata, heat flux: 2×10^4~5×10^6 kcal/m^{2}h, mass velocity: 40~5400 kg/m^{2}s. The number of experimental data for the pressure of 140 ata in reference (8) is small, and the boundaries of flow patterns can not be defined. The data for the pressures of 10 ata to 98 ata, therefore, are used to map the flow patterns.

For a vertical two-phase flow, the flow patterns classified by different authors are as follows,

i) Bergles, et al.[3),4)] : Bubble, slug, froth, annular dispersed, and dispersed flow.

ii) Bennett, et al.[7)] : Bubble, slug, churn, annular, and wispy annular flow.

iii) Fiori, et al.[5)] : Bubble, slug, annular, and annular dispersed flow.

iv) Hosler, et al.[8)] : Bubble, slug, and annular flow.

Dispersed flow is defined as one of complete dispersion of the liquid in the gas without a liquid film on the channel wall.

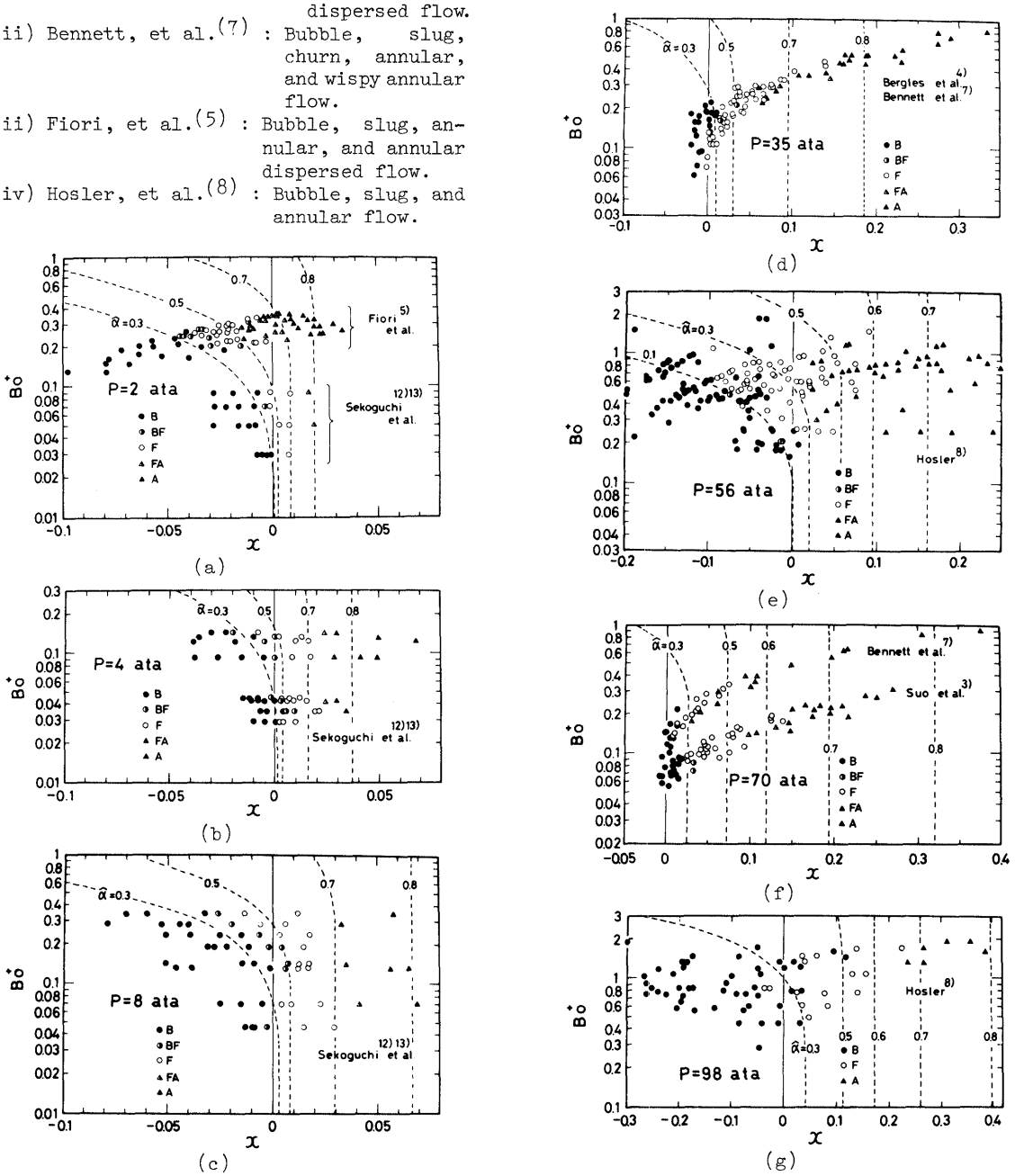

Fig.7 Flow pattern map on Bo^+ vs. x

Table 1 Range of experimental parameters used for mapping flow patterns

Investigator	Sekoguchi et al.[12),13)]	Suo et al.[3)]	Bennett et al.[7)]	Fiori et al.[5)]	Bergles et al.[4)]	Hosler et al.[8)]
Fluid	Steam - water system					
Flow direction	Vertical upward flow					
Channel geometry and dimension, mm	circular ϕ11~16	circular ϕ10.16	circular ϕ12.7	circular ϕ2.4~6.1	circular ϕ10	rectangular 3.4×25.4
Pressure, ata	1~16	70	35,70	2~7	35,70	10~140
Heat flux, kcal/m²h	2×10^5 ~1.4×10^6	8×10^5 ~1.6×10^6	4.4×10^5 ~1.1×10^6	2×10^5 ~5×10^6	3×10^5 ~4×10^6	10^5 ~5×10^6
Mass velocity, kg/m²s	310~2000	540~2700	40~400	270~3300	540~5400	130~5400
Determination technique of flow patterns	Probe technique	Visual observation and Probe technique	Visual observation and X-ray photograpy	Visual observation and Probe technique	Visual observation and Probe technique	Visual observation

Churn flow is sometimes referred to as another name of froth flow. Wispy annular flow takes the form of a relatively thick liquid film on the wall of the pipe together with a considerable amount of liquid entrained in a central gas or vapor core. The liquid film is aerated by small gas bubbles and the entrained liquid phase appears as large droplets which have agglomerated into long irregular filaments or wisps.

In this paper, flow patterns in boiling flow are divided into three categories of bubble, froth which combines a slug and a churn flow, and annular flow which includes an annular dispersed flow. Considering that the wispy annular flow seems to have the common properties of the froth and the annular flow, the wispy annular flow is treated as the transition between these two flows.

As can typically be seen from Figs.7 (a) and (e), the transition boundary from bubble to froth flow is clearly in the same tendency as the constant average void fraction curves drawn by dotted lines. This suggests that the average void fraction can reasonably serve as a criterion for classification of flow patterns.

Two void fractions corresponding to the transitions from bubble to froth flow and from froth to annular flow are plotted against pressure in Fig.8. Although the classification systems employed by the researchers listed in Table 1 may be somewhat different from each other, $\hat{\alpha}$-values of the transitions fit into relatively narrow bands ; i.e., $\hat{\alpha}=0.2\sim0.4$ for the transition from bubble to froth flow, and $\hat{\alpha}=0.6\sim0.8$ for the transition from froth to annular flow. However, the void fraction for each transition decreases as the pressure increases. This can be expressed as a function of pressure by the following equation;

$$\hat{\alpha}=a-0.022\ln(p/p_c) \quad \cdots\cdots(15)$$

where, P_c is the critical pressure of water, and a is a constant. The values of a for the two transitions are 0.28 and 0.63, respectively.

Figure 9 is a general flow map based on the criteria of Eq.(15) by taking Bo^+ and x as the coordinates and pressure as a parameter. The solid lines show the transition from bubble to froth flow, and the dotted lines do the transition froth to annular flow. The experimental conditions covered by the present correlation are pressure: $1\sim98$ ata, heat flux: $2\times10^4\sim5\times10^6$ kcal/m^{2}h, mass velocity: $40\sim5400$ kg/m^{2}s, and channel geometry: circular or rectangular.

It was shown in our paper(2) that experimental results of void fractions for

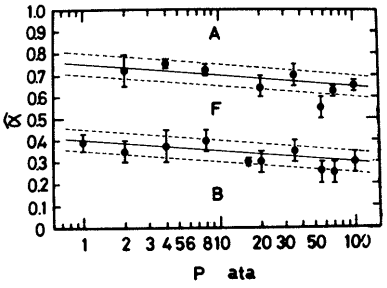

Fig.8 Effect of pressure on average void fractions for flow pattern transitions

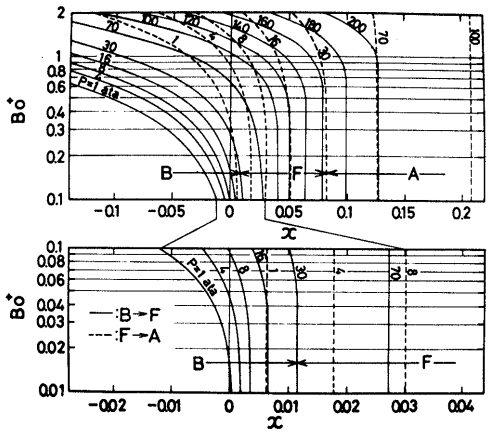

Fig.9 Flow pattern map

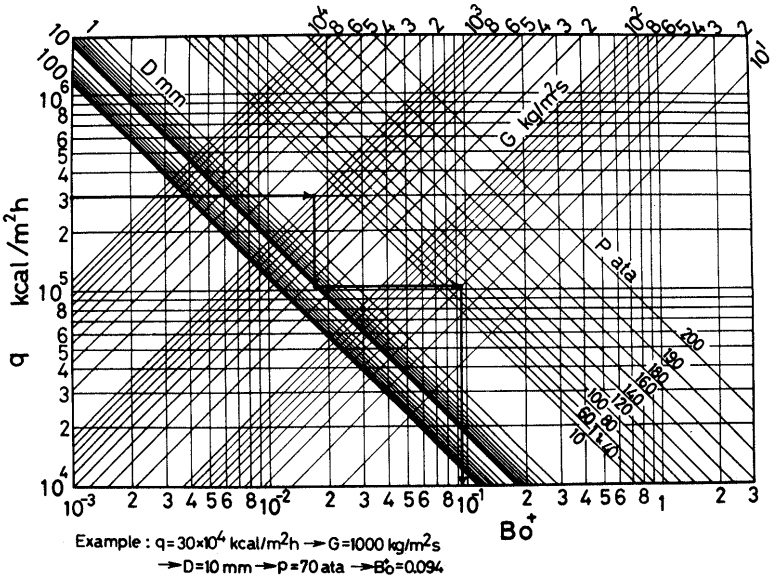

Fig.10 Calculation chart of Bo^+

various channel geometries such as circle, rectangle, and annuli are in good agreement with those calculated by the authors' prediction method of void fraction, from which an important parameter Bo^+ for mapping flow regimes is introduced. Therefore, the flow map proposed here is probably effective not only for circular and rectangular channels, but for annular channel. For convenience of using the flow map, a culculation chart for Bo^+ is given in Fig.10.

The flow patterns are largely divided into three regimes of bubble, froth and annular flow in this study. As thermal-hydrodynamic mechanisms of boiling flow are made clear, much more precise or improved classification will probably be developed. For example, the adiabatic two-phase annular flow has already been subdivided into minor flow regimes depending upon the characteristics in liquid phase behavior. Thus, more detailed measurements of the liquid phase behaviors of a boiling flow should be performed to clarify the interrelationship between transfer mechanisms of momentum and heat with flow patterns.

7. Conclusions

An instrument technique of void fraction profile is applied to classifying the flow patterns in the subcooled and flow quality boiling regions. Next, a newly developed flow map is proposed using a parameter derived from the prediction method of void fraction, which has been presented in our previous report(2). The results obtained from this study are summarized as follows.

(1) Flow pattern boundary decided from void fraction profiles uniquely corresponds to a specific value of the void fraction averaged through a cross section of the channel.
(2) Flow patterns such as bubble, froth and annular flow can simply be mapped with thermal equilibrium quality, x, and a new parameter, Bo^+, consisting of heat flux, mass velocity, pressure, and equivalent diameter of channel. The transition boundaries on the flow map are reasonably consistent with experimental data of a boiling flow available in the literature and our data, which cover the following experimental conditions of pressure: 1~98 ata, heat flux: 2×10^4~5×10^6 kcal/m^{2}h, and mass velocity: 40~5400 kg/m^{2}s.
(3) Both the specific values of void fraction, at which the transitions occur from bubble to froth flow, and from froth to annular flow, decrease with increasing pressure.
(4) A general flow map for a boiling flow is obtained by taking the pressure as a parameter.

Acknowledgements

The authors wish to thank Kyushu University Computation Center for calculation of experimental data, and the Education Ministry for their support in part of this work (The Science Research Fund 1979, Title number (A) 335010)

References

(1) Sekoguchi, K., Aspects of Advanced Heat Transfer (in Japanese), Vol.1 (1973), p.217, Yokendo.
(2) Sekoguchi, K., et al., Bull. JSME, Vol.23, No.183 (1980-9), p.1475.
(3) Suo, M., et al., Dynatech Rep. NYO-3304-3 (1965).
(4) Bergles, A.E. and Suo, M., Dynatech Rep. NYO-3304-8 (1966).
(5) Fiori, M.P. and Bergles, A.E., M.I.T. Rep., No.5382-40 (1966).
(6) Sekoguchi, K., et al., Proc. 5th Int. Heat Transf. Conf., Vol.4 (1974-9), p.180.
(7) Bennet, A., et al., AERE R4874 (1965).
(8) Hosler, E.R., Westinghouse Electric Corp., Atomic Power Division, WAPD-TM-658 (1967).
(9) Sekoguchi, K. et al., Bull. JSME, Vol.19, No.128 (1976-2), p.187.
(10) Radovcich, N.A. and Moissis, R., Dept. Mech. Engng., M.I.T. Rep., No.7-7673-22 (1969).
(11) Sekoguchi, K., Preprint of 404th Lecture of JSME (in Japanese)(1975-4), p.53.
(12) Sekoguchi, K., et al., Proc. 9th Symp. Heat Transf. Japan (in Japanese)(1972-5), p.17.
(13) Sekoguchi, K., et al., Proc. 10th Symp. Heat Transf. Japan (in Japanese) (1973-5), p.1.
(14) Jones, O. C. and Zuber, N., Int. J. Multiphase Flow, Vol.2 (1975), p.273.
(15) Smith, S.L., Proc. Inst. Mech. Engr., Pt 1, Vol. 184, No. 36 (1969-1970), p.647.
(16) Bowring, R.W., OECD Halden Reactor Project Report, Norway, HPR-10, (1962), p.88.
(17) Levy, S., Int.J. Heat & mass Transf., Vol.10, No.7 (1967-7), p.951.
(18) Kroeger, P.G. and Zuber, N., Int. J. Heat & Mass Transf., Vol.11, No.2 (1968-2), p.211.
(19) Larsen, P.S. and Tong, L.S., Trans. ASME, Ser.C. Vol.91, No.4 (1969-11), p.471.
(20) Ahmad, S.Y., Int. J. Heat & Mass Transf., Vol.92, No.4 (1970-11), p.595.
(21) Rouhani, S.Z. and Axelsson, E., Int. J. Heat & Mass Transf., Vol.13, No.2 (1970-2), p.383.
(22) Bartolemei, G.G. and Chanturia V.M., Teploenergetika, Vol.14, No.2 (1967-2), p.80.
(23) Maurer, G.W., Westinghouse Electric Corp., Atomic Power Division, WAPD-BT-19 (1960), p.59.
(24) Christensen, H., Argonne Nat. Lab., ANL-6385 (1961).
(25) Egen, R.A., et al., Battelle Memorial Institute, BMI-1163 (1957).
(26) Rouhani, S. Z., Aktiebolaget Atomenergi, Sweden, AE-239 (1966).
(27) Foglia, J.J., et al., Battelle Memorial Institute, BMI-1517 (1961), p.28.
(28) Martin, R., Nucl. Sci. & Engng., Vol. 48, No.2 (1972-6), p.125.